# Influence of the Print Process on the Durability of Printed Cementitious Materials

Jolien Van Der Putten(✉) , M. De Smet, P. Van den Heede , Geert De Schutter ,
and Kim Van Tittelboom

Magnel-Vandepitte Laboratory for Structural Engineering and Building Materials, Ghent University, Tech Lane Ghent Science Park, Campus A Building 60, 9052 Ghent, Belgium
Jolien.VanDerPutten@UGent.be

**Abstract.** 3D concrete printing (3DCP) is currently being explored both in academia and practice and ensures a fast, economic, safe and formwork-free construction process. Although the elimination of formwork is one of the biggest advantages, it also removes the protection between the curing concrete and the surrounding environment and consequently, cracking resulting from shrinkage can be more pronounced. Additionally, the effect of the layered fabrication process and the absence of compaction could increase the porosity and the occurrence of weakly bonded interfaces. The combination of these three phenomena might affect the durability of 3DCP elements, as these interfaces form ideal ingress paths for chemical substances. In order to improve the long-term behavior, this study aimed to comprehend the correlation between different print process parameters and the resistance against carbonation. Therefore, multi-layered elements were fabricated with two different print techniques (2D and 3D) and two interlayer time gaps (0 and 30 min). To enable a complete comparison between both fabrication processes also conventional cast elements were considered. In general, a more pronounced $CO_2$ penetration could be observed for printed elements, related to the higher porosity. Additionally, enlarged time gaps tend to be detrimental for the durability, however, this effect could be counteracted the 3D-print technique. The higher pump pressure improves the bonding between subsequent layers and the general long-term behavior.

**Keywords:** 3D printing · Carbonation resistance · Durability

## 1 Introduction

With an annual production of six billion ton, concrete can be considered as the most widely used and most important construction material nowadays [1]. Even though the material science has been progressing rapidly, the improvements made in the manufacturing process are limited; the construction process is still labor intensive, the fabrication of molds and the integration of reinforcement is time consuming, especially when the complexity of the design increases. Therefore, additive manufacturing (AM), defined as 'the process of joining materials to make objects from 3D model data, usually layer upon layer' is gaining ground in the construction industry [2]. The most popular AM-technique

is 3D concrete printing (3DCP). This method allows a fast, economic, safe and formwork-free construction process with more architectural design freedom. Notwithstanding the many advantages of 3DCP, the layered end process could result in a higher porosity and the occurrence of weakly bonded interfaces [3, 4]. Additionally, the elimination of formwork goes along with the removal of the barrier between the curing concrete and the surrounding environment which could lead to more pronounced shrinkage related cracking [5]. These cracks, the higher porosity and the weakly bonded interfaces will not only weaken the structural properties of the elements, but might also affect the durability as they form ideal ingress paths for chemical substances [6]. At this moment, the addition of reinforcement is still an issue. However, once this will become daily practice, different corrosion-inducing mechanisms will become a threat and the transport properties and durability aspects will become of major importance. A typical deterioration mechanism associated with reinforced concrete structures is carbonation, decreasing the alkalinity of the concrete due to the reaction of $CO_2$ with various hydrates. This study therefore aims to comprehend the correlation between the applied print parameters (i.e. print process and interlayer time gap) and the durability of the cementitious material. In addition, a comparative study between printed and cast elements is made.

## 2   Materials and Methods

### 2.1   Materials and Mix Composition

The printable mixture was composed out of Portland Cement (CEM I 52.5 N) in combination with siliceous sea sand (0/2), water (W/C = 0.37) and a polycarboxylic ether-based superplasticizer (SP) (Glenium 51, conc. 35%, BASF, Germany). The mix composition can be found in Table 1.

**Table 1.** Mix composition

| Component | CEM I 52.5 | Sea sand | Water | SP |
|---|---|---|---|---|
| Amount [kg/m$^3$] | 703 | 1055 | 257 | 0.47% (woc) |

### 2.2   Print Process and Sample Preparation

A Quick-point mortar extruder, mounted vertically on a fixed steel frame, was used to simulate an extrusion-based print process (Fig. 1A). The mortar extruder could be manually altered in height to ensure a proper clearance between the nozzle and the building platform. The extrusion nozzle was elliptically shaped (28 × 18 mm$^2$). The extruder is able to print layers up to 300 mm length, with different printing speeds. Within the scope of this research, a printing speed equal to 1.7 cm/s was selected. The width and height of the printed layers equaled 28 mm and 10 mm, respectively. Specimens printed with this technique will be denoted as 2D-printed samples.

The upscaled 3D print experiments were executed with a six-axis industrial robot (Fig. 1B). The fresh cementitious material was transported to the print head with a progressive screw-based pump, connected to a 5 m long rubber hose. The layers were extruded with an elliptical nozzle ($33 \times 20 \text{ mm}^2$) at a print velocity of 15 cm/s. The width and height of the printed layers equaled 33 mm and 10 mm, respectively. Specimens printed with this technique will be denoted as 3D-printed samples. Irrespective of the applied printing process, sample preparation starts by extruding the cementitious material through the nozzle with a predefined velocity. For each sample a single base layer was extruded. After a predefined time gap (zero or 30 min, denoted as T0 or T30, respectively), a second layer was deposited on top of the previous one, starting at the same initial X-position to ensure an equal time gap along the entire specimen. This process was repeated until four-layered samples were obtained. After printing, specimens were cured in standardized conditions ($20 \pm 2$ °C, $60 \pm 5\%$ RH) until the day of testing.

The resistance against carbonation of printed specimens was compared with mold-cast elements, denoted as CAST. Therefore, prismatic molds ($160 \times 40 \times 40 \text{ mm}^3$) were filled with mortar in two steps and compacted on a jolting table by 60 jolts. These molds were then covered with plastic foil and stored in standardized conditions ($20 \pm 2$ °C, $60 \pm 5\%$ RH). After 24 h, the prisms were demolded and stored in the same environment until the day of testing.
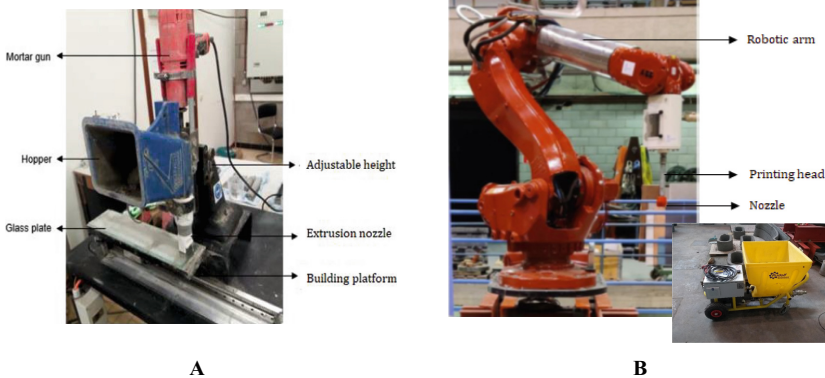


**Fig. 1.** Small-scale mortar extruder (A) and six-axis 3D-printing robot with pump (B).

## 2.3 Carbonation Resistance

The carbonation resistance was investigated according to the standard CEN/TS 12390-10. To start the procedure, printed and mold-cast specimens were sawn into smaller elements with dimensions as depicted in Fig. 2A and 2B. Thereafter, 5 of the 6 sample sides were coated with an epoxy resin (Episol Designtop SF – Resiplast, Fig. 2C) to ensure unidirectional $CO_2$ transport through the non-coated front surface. At the age of 12 days, these coated elements were stored in a carbonation chamber at 20 °C and 60% RH containing 1 vol% $CO_2$. Due to the specimens age at the start of the $CO_2$

exposure, this procedure deviates from the one specified in the standard, but can be explained as follows. In general, the carbonation front proceeds when all the material is carbonated. Due to the higher binder content in printable mixtures and as Portland cement is the only binder component, the amount of carbonatable material is high. Assuming that the carbonation front would proceed slowly, specimens were therefore placed in the carbonation chamber after a hardening period of 12 days. After a $CO_2$ exposure of 1, 3, 5 and 7 weeks, a minimum of 3 samples per test series was split perpendicular to their non-coated surface. The carbonation front was visualized by spraying a 1% phenolphthalein solution on these freshy split surfaces, where the non-carbonated region turns into a characteristic magenta color as this region is still highly alkaline. After photographing the split surfaces, ImageJ analysis was performed to measure the carbonation depth every millimeter as a function of time. Side effects were excluded as only the second and third layer were considered within the investigations.
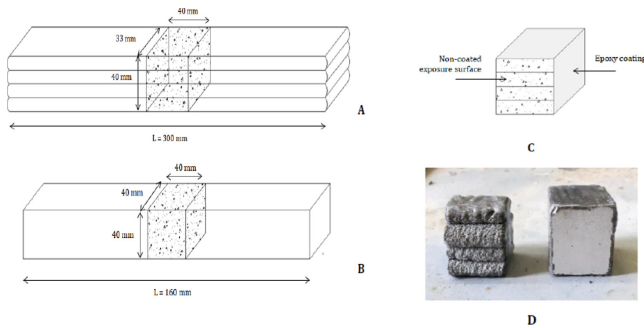


**Fig. 2.** Schematic representation of a four-layered printed element (A) and a traditionally cast specimen (B), schematic representation of the sample preparation indicating the coated and non-coated surfaces (C) and the prepared samples (D)

## 3   Results and Discussion

Based on the colorimetric visualization of the carbonation front and subsequent ImageJ analysis, the penetration of $CO_2$ can be expressed as a function of time (Fig. 3A–E). The latter figures visualize the carbonation front over the specimen's height, where the X-axis represents the position of the interlayer between the second and third layer. Comparing different manufacturing processes, one can conclude that printed specimens show a lower resistance against $CO_2$ ingress. After one week of exposure, the carbonation front penetrated only $1 \pm 0.01$ mm into the cast samples, while in case of printed specimens approximately $5 \pm 0.45$ mm of the bulk material was carbonated, regardless of the print technique. This can be attributed to the higher porosity and the higher shrinkage related (micro-)cracks formed due to the lack of molding [6]. Both phenomena increase the amount of preferential ingress paths for chemical substances. In case of traditional mold-cast elements, the penetration front is straight and uniform over the entire height, highlighting the homogeneity of the material. When the applied time gap equals zero, a

similar shape of the carbonation front can be observed for both print techniques. Although the penetration depth is higher ($\pm200\%$ higher in case of printed samples after one week of $CO_2$-exposure), the printable material can also be assumed as homogenous when the layers are printed directly upon each other. Enlarged time gaps induce preferential ingress paths at the interlayer, especially in case of 2D-printed elements (Fig. 3E). The latter phenomenon can be attributed to the decreased interlayer quality. The higher the time gap between the layers, the drier the substrate material and the lower the interlayer bonding [4, 6]. This effect seems to be counteracted by the higher pressure executed when making use of the 3D printing technique. As both the preferential ingress at the interlayer and the penetration depth in general are lower compared to 2D-printed elements, one can conclude that the application of the 3D printing technique enhances the long-term behavior of the specimens.
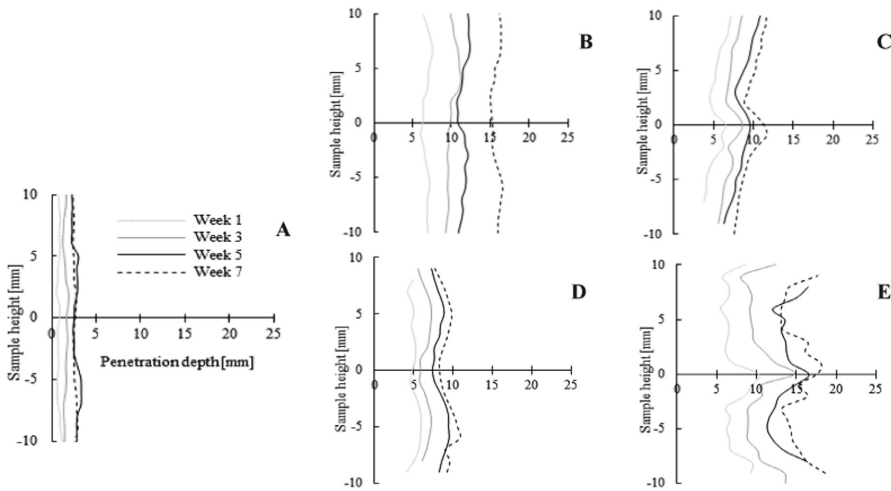


**Fig. 3.** $CO_2$ ingress in case of traditional cast elements (A), 3D-elements fabricated with a zero (B) or 30-min time gap (C) and 2D-elements with a zero (D) or 30-min time gap (E) ($n = 3$, error bars are left out for the sake of clearance).

For each test series, the measured carbonation depths [mm] were plotted as a function of the square root of the exposure time [weeks] to determine an experimental carbonation coefficient $A_{cc}$ [mm/$\sqrt{}$weeks]. The results of the latter are represented in Fig. 4 and confirms the conclusions mentioned above.

$A_{cc}$ is the lowest in case of mold-cast samples due to the higher compaction degree and the lower porosity. Higher time intervals result in a higher carbonation coefficient, as observed for 2D-printed elements, and the detrimental effect of an enlarged time gap can be counteracted by the 3D print technique. The higher carbonation coefficient in case of 3D-printed elements can be related to the environmental conditions. Although the specimens were stored in climatized conditions, they were manufactured in non-standardized lab conditions. The lower temperature and RH during the first hours after printing could enlarge the early-age drying process and result in a higher (micro)crack formation. Considering mold-cast specimens as the reference, one can conclude that
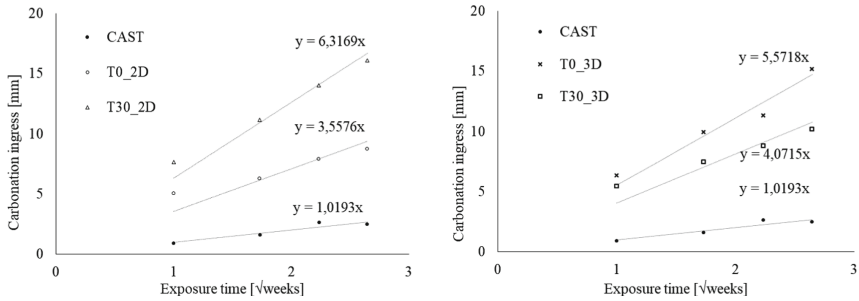
**Fig. 4.** Carbonation coefficient in case of different manufacturing techniques (CAST, 2D or 3D) and different time gaps (T0 and T30)

the resistance against carbonation is inadequate and the material would result in corrosion of eventual embedded reinforcement. To improve the long-term behavior, print process parameters or the material composition can be adapted. Another possibility is the application of adequate curing methods. All this would limit the desiccation of the outer layers and lower their porosity, impeding the diffusion of $CO_2$ and slowing down the carbonation process.

## 4   Conclusions

Based on the current investigation, one can conclude that the manufacturing process and the individual print parameters (e.g. interlayer time gap) will not only affect the structural behavior, but also the long-term durability behavior. Due to the higher compaction degree and the lower porosity, traditional manufactured elements carbonate less compared with printed elements. When the interlayer time gap equals zero, the carbonation front is uniform, irrespective of the applied fabrication technique. Enlarged time gaps increase the preferential ingress paths due to the lower surface quality of the substrate layer. However, the higher print pressure in case of 3D printing is able to counteract the latter phenomenon.

## References

1. De Schutter, G., et al.: Vision of 3D printing with concrete — technical, economic and environmental potentials. Cem. Concr. Res. **112**, 25–36 (2018)
2. Bos, F., et al.: Additive manufacturing of concrete in construction: potentials and challenges of 3D concrete printing. Virt. Phys. Prototyp. **11**(3), 209–225 (2016)
3. Nerella, V.N., Hempel, S., Mechtcherine, V.: Effects of layer-interface properties on mechanical performance of concrete elements produced by extrusion-based 3D-printing. Constr. Build. Mater. **205**, 586–601 (2019)
4. Van Der Putten, J., Deprez, M., Cnudde, V., De Schutter, G., Van Tittelboom, K.: Microstructural characterization of 3D printed cementitious materials. Materials **12**(18), 2993 (2019)
5. Buswell, R.A., et al.: 3D printing using concrete extrusion: a roadmap for research. Cem. Concr. Res. **112**, 37–49 (2018)
6. Van Der Putten, J.: Mechanical Properties and Durability of 3D Printed Cementitious Materials, in Faculty of Engineering and Architecture, Ghent University, Ghent (2021)